

Thermoelectric Generators as Alternative Source for Electric Power

L. C. Ding, Bradley. G. Orr, K. Rahaoui, S. Truza, A. Date, A. Akbarzadeh

Abstract—The research on thermoelectric has been a blooming field of research for the latest decade, owing to large amount of heat source available to be harvested, being eco-friendly and static in operation. This paper provides the performance of thermoelectric generator (TEG) with bulk material of bismuth telluride, Bi_2Te_3 . Later, the performance of the TEGs is evaluated by considering attaching the TEGs on a plastic (polyethylene sheet) in contrast to the common method of attaching the TEGs on the metal surface.

Keywords—Electric power, heat transfer, renewable energy, thermoelectric generator.

I. INTRODUCTION

As proposed by [1], thermoelectrics will able to provide a significant role as the alternative source of electric energy as long as the cost could be reduced and there is an improvement of thermal-electric conversion efficiency. In order to facilitate the thermal-electric conversion, heat is supplied at the hot junction of the thermoelectric generator (TEG) and the heat is removed at cold junction in order to create a temperature difference across the hot and cold junction. To date, numerous studies has been carried out, with different types of heat source and heat sink, e.g. hot exhaust air [2]–[4], hot water [5], air cooled or water cooled [6], [7].

From the aforementioned research conducted, the TEGs are attached to a surface of highly conductive material and often, on the surface of a metal plate as to provide a barrier for the mixing of hot and cold fluid and yet providing a good heat conduction. This paper will explore a slightly different approach, which considering the use of plastic to replace the use of metal in order to attach the TEG. Despite having a low thermal conductivity (e.g. polyethylene with thermal conductivity, k of $0.35 \text{ W/m}^\circ\text{C}$ compared with aluminium with $k = 205 \text{ W/m}^\circ\text{C}$), plastic offer a relatively thinner thickness (range from $30\text{--}100\mu\text{m}$) and advantage of lighter weight and lower in cost. Hence, its unfavourable lower heat conductivity is compensated by its relatively thin thickness compared with metal. As a result, the difference in the thermal resistance exerted by plastic is about 30 times compared with aluminium (assuming polyethylene sheet of $50\mu\text{m}$ and aluminium sheet thickness of 1mm).

L. C. Ding is PhD candidate at Royal Melbourne Institute of Technology, Melbourne, Australia (e-mail: laichet.ding@rmit.edu.au).

Bradley.G. Orr, K. Rahaoui, S. Truza, A. Date, and A. Akbarzadeh are Energy CARE group members at School of Aerospace, Mechanical and Manufacturing Engineering in Royal Melbourne Institute of Technology, Melbourne, Australia.

II. THE THERMOELECTRIC GENERATOR

A. Fundamental

Seebeck effect is the main effect that lies behind the working principle of a thermoelectric generator (TEG). Seebeck effect is a phenomenon where electromotive force (EMF) is generated when two dissimilar metals connected together and subjected to heat at one of the connecting junction (Fig. 1).

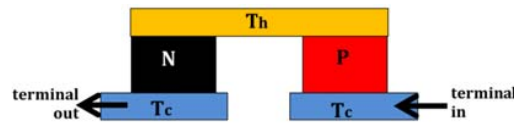


Fig. 1 A pair of P-N legs coupled electrically in series and thermally in parallel

Under a given load resistance of R_L , and TEG internal resistance of R , the power generated by the TEG is $\dot{W} = I^2 R_L$ and the conversion efficiency of the TEG is:

$$\eta_t = \frac{\dot{W}}{\dot{Q}_h} = \frac{I^2 R_L}{\alpha T_h I - \frac{1}{2} I^2 R + K(T_h - T_c)} \quad (1)$$

In an open circuit, the voltage generated (incorporating both load resistance and the resistance by the wiring) is, hence:

$$V_{oc} = \alpha \Delta T = \alpha(T_h - T_c) = I(R_L + R) \quad (2)$$

By referring to (1) and (2), the power generated, \dot{W} by the TEG can be represented by:

$$\dot{W} = \left(\frac{\alpha \Delta T}{R_L + R} \right)^2 \frac{R_L}{R} \quad (3)$$

From (2), $V_{oc} = \alpha \Delta T = \alpha(T_h - T_c)$ and the maximum power produced by the TEG for a given ΔT will be $\dot{W}_{max} = \frac{V_{oc} I_{sc}}{4}$ where V_{oc} and I_{sc} are the open circuit voltage and short circuit current. By using the relation of $V = IR_L$, the maximum power happens at $R_L = R$, which gives:

$$\dot{W}_{max} = \frac{\left(\frac{V_{oc}}{\Delta T} \right)^2 \Delta T^2}{4R} \quad (4)$$

Since a typical voltage-current and power-current relation for the TEG is in linear and parabolic forms, respectively, as illustrated in Fig. 2.

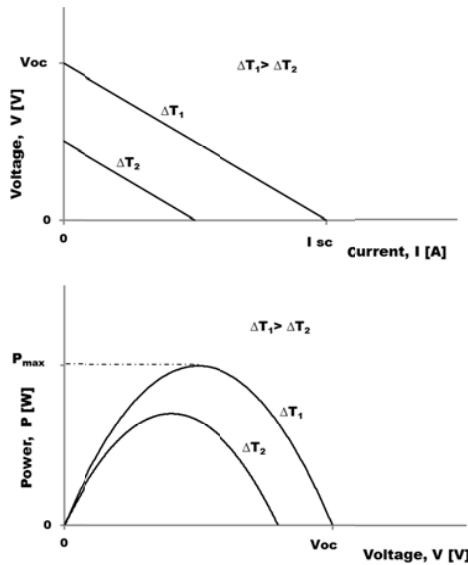


Fig. 2 Typical voltage-current and power-voltage curve for TEG

B. Single TEG Laboratory Testing

The testing of the TEG was conducted by exposing the hot side of the TEG to the heat provided by the cartridge heater, being controlled using a variable power supply and water cooled by a cooler. The electrical loading in the circuit was supplied by an electronic load. The electric resistance tested in current testing ranges from 0Ω to 4000Ω . The TEG used in this study is a commercially available bulk material of Bi_2Te_3 with the dimension of $40\text{ mm} \times 40\text{ mm}$ (consists of 127 pair of P-N legs). The layout of the testing schematic is shown in Fig. 3.

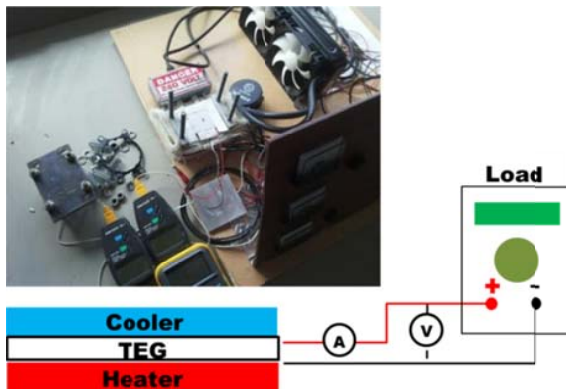


Fig. 3 The single cell TEG testing layout

Figs. 4 and 5 show the result of the TEG testing with hot side temperature, T_h of 86°C and cold side temperature, T_c of 30°C . At the load matching condition where $R_L = R$, 1.0 W of electric power had been produced. Furthermore, different temperature difference had been tested by varying the input power of the heater. As a result, different temperature differences were created across the hot and cold junction of the TEG and the result, are shown in Fig. 6. The shaded region in Fig. 6 represents the maximum power produce by the TEG under different temperature difference, ΔT . From Fig. 7, maximum

power produced by the TEG at ΔT of 46°C was 0.87 W, whereas at ΔT of as low as 11°C , 0.08 W of electric power had been produced. Besides testing the TEG of its performance characteristic curve, another important parameter in the thermal modeling, which is the thermal resistance of the TEG was evaluated. As depicted in Fig. 7, the TEG used in this study has a fairly constant thermal resistance of $0.6^\circ\text{C}/\text{W}$, for the range of ΔT tested. Both the electric and thermal performance established from the single TEG testing will be used in the evaluation of the TEG performance (in the next section) when it incorporates with plastic (polyethylene with thickness of $70\mu\text{m}$), and hence replacing steel plate (which is the most commonly used method).

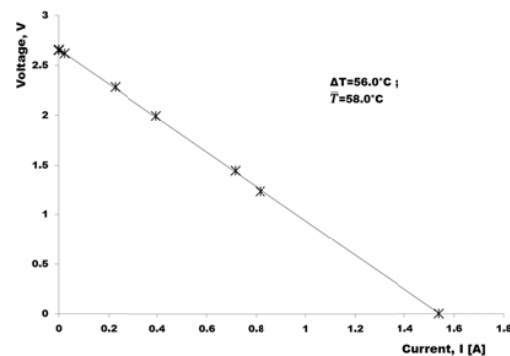


Fig. 4 Voltage-current graph for single TEG

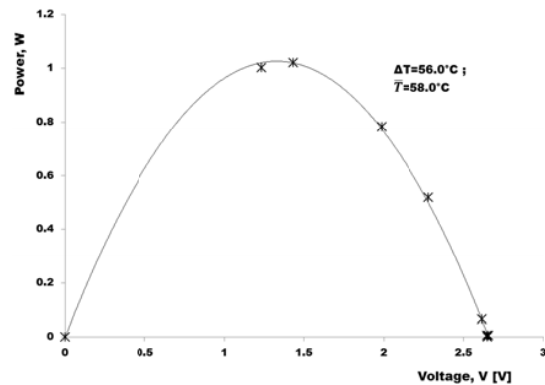


Fig. 5 Power-voltage curve for single TEG

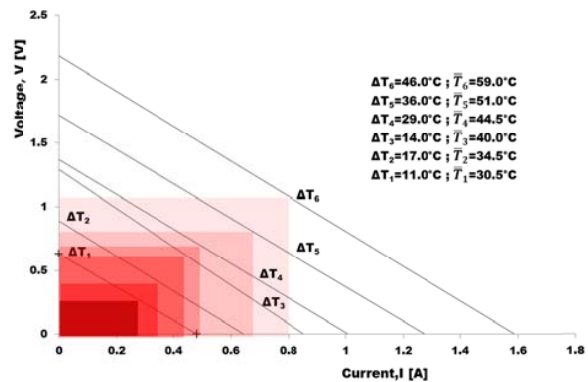


Fig. 6 Voltage-current graphs with different temperature difference

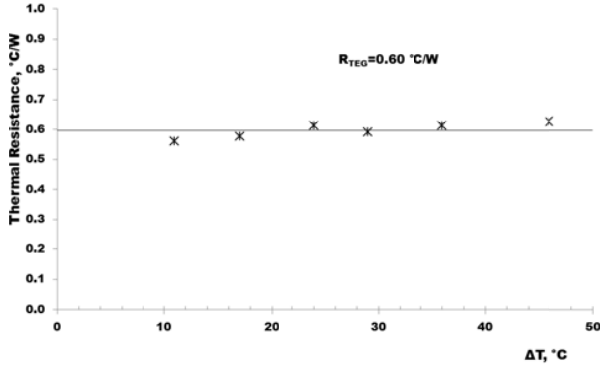


Fig. 7 Thermal resistance of single TEG with temperature difference

III. THE PLASTIC (POLYETHYLENE)-TEG COMBINATION

A. Theory

The proposed design shown in Fig. 8 consists of a total of 12

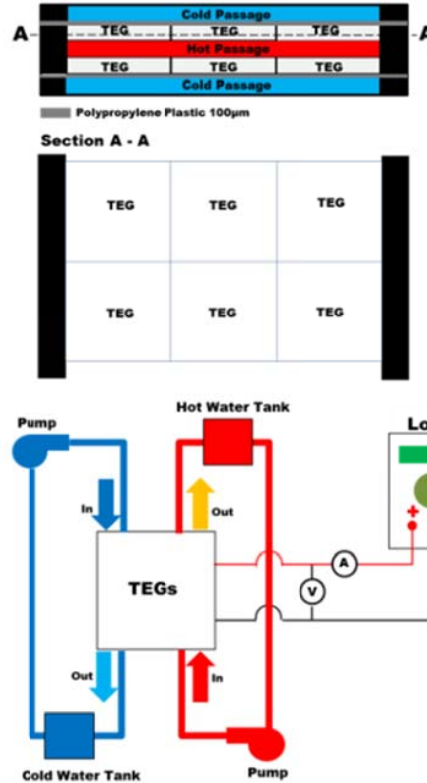
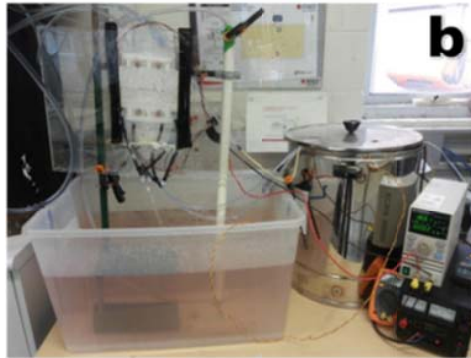
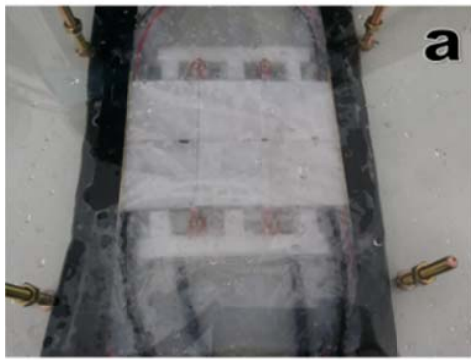


Fig. 8 System schematic

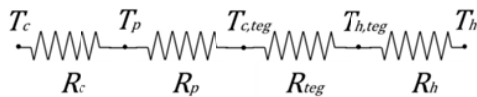


Fig. 9 Thermal resistant network

The thermal properties of water which are thermal conductivity, k_w , density, ρ_w , and specific heat capacity, c_w are calculated based on the following relations. For fresh water, S

TEGs, with 6 TEGs at each layers. Hot water will circulate through the channel sandwiched by outer cold water channels, as shown in (a). Imposing symmetry on the design, we have:

$$\dot{Q} = \dot{m}_c c_{p,c} (T_{c,out} - T_{c,in}) = \frac{1}{2} \dot{m}_h c_{p,h} (T_{h,in} - T_{h,out}) = \frac{T_{h,out} - T_{c,in}}{\sum R} = \frac{T_{h,in} - T_{c,out}}{\sum R} \quad (5)$$

Using thermal resistance network method (as shown in Fig. 9), we will able to solve the unknown, which are $T_{c,out}$ and $T_{h,out}$.

$$\sum R = R_c + R_{teg} + R_p + R_h$$

$$R_{teg} = 2R_{TEG}/N$$

$$\Delta T_{TEG} = T_{h,teg} - T_{c,teg} = \frac{\dot{Q}}{R_{TEG}}$$

which refers to salinity in g/kg is equivalent to zero and the unit T refers to fluid temperature.

$$k_w = 0.5553 - 0.0000813S + 0.0008(T - 20) \quad (6)$$

$$\rho_w = 998 + 0.65S - 0.4(T - 20) \quad (7)$$

$$c_w = 4180 - 4.396S + 0.0048S^2 \quad (8)$$

The hydraulic diameter of the water passage is calculated via:

$$D_h = \frac{4wb}{2(w+b)} \quad (9)$$

and its corresponding Reynolds number are evaluated:

$$Re_c = \frac{\rho_c \dot{V} D_h}{\mu_c w_c b} \quad (10)$$

$$Re_h = \frac{\rho_h \dot{V} D_h}{\mu_h w_h b} \quad (11)$$

For developed turbulent flow, the Nusselt number is calculated using commonly adopted Dittus-Boelter equation $Nu = 0.023 Re^{0.8}$ where $n=0.3$ for hot side and $n=0.4$ for cold side. If the Reynolds number is less than 2300, then the Nusselt number, Nu is equal to 4.36. Later, the convection heat transfer coefficient is calculated by:

$$h = \frac{Nu \cdot k}{D_h} \quad (12)$$

B. Theoretical Performance

The input values assigned for the theoretical analysis are listed in Table I.

TABLE I
INPUT VALUES

Input	Value
$T_{c,in}$	10 °C
$T_{h,in}$	90 °C
b	$3 \times a = 120 \text{ mm}$
R_p	$R_p = \left(\frac{l}{kA}\right)_p$ with thickness $l=70\mu\text{m}$, $k=0.35\text{W/m}^\circ\text{C}$, and area, $A = \frac{N}{2}a^2 = 6 \cdot 40^2 \text{ mm}^2$
R_{TEG}	0.6 °C/W

From the theoretical modeling, at $T_{c,in}$ of 10°C and $T_{h,in}$ of 90 °C, by using 12 TEGs arranged as shown in Fig. 8, 17.2 W of electrical power will be able to be generated as shown in Fig. 11 with the corresponding ΔT_{TEG} illustrated in Fig. 10.

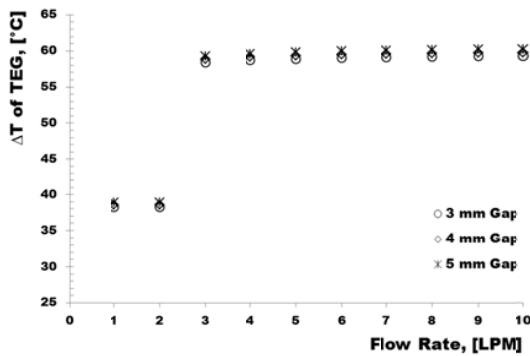


Fig. 10 Temperature difference across TEG with regard to flow rate and gap size

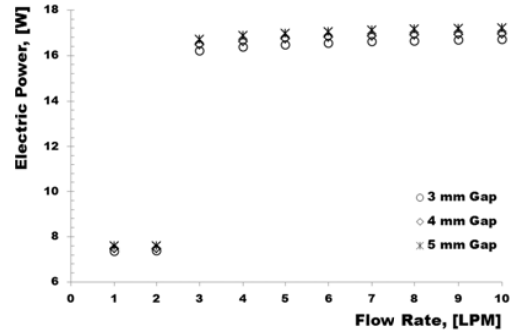


Fig. 11 Electric power with regard to flow rate and gap size

C. Experimental Testing

The testing was carried out by supplying the hot water at 50°C with a flow rate of 1.4 LPM passing through a gap of 4 mm whereas the cold water was supplied into 4 mm cold water passage at 15°C with a flow rate of 0.5 LPM. The layout for the testing is as shown in Fig. 8 (b). The ambient temperature during the testing was 14°C. Fig. 12 summarizes the testing result.

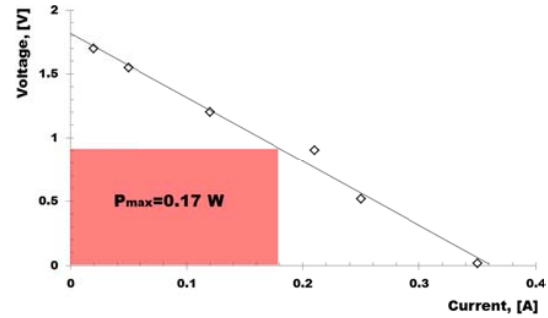


Fig. 12 Testing result

From the testing conducted, 0.17W of electrical power can be produced at the aforementioned low flow rate and incoming fluid temperature difference as low as 35°C.

IV. CONCLUSION

This paper has presented the testing and performance of a commercially available bismuth telluride, Bi_2Te_3 TEG. Later, the performance of the TEGs when they couple with plastic is analyzed. The result had shown the potential of generating electric power under plastic-TEGs combination.

REFERENCES

- [1] D.M. Rowe, "Thermoelectrics, an environmentally-friendly source of electrical power," in *Renewable Energy*, vol 16, Issues 1–4, pp.1251-1256, January–April 1999.
- [2] Byung deok In, Hyung ik Kim, Jung wook Son, Ki hyung Lee, "The study of a thermoelectric generator with various thermal conditions of exhaust gas from a diesel engine," in *International Journal of Heat and Mass Transfer*, vol. 86, pp. 667-680, July 2015.
- [3] Hongliang Lu, Ting Wu, Shengqiang Bai, Kangcong Xu, Yingjie Huang, Weimin Gao, Xianglin Yin, Lidong Chen, "Experiment on thermal uniformity and pressure drop of exhaust heat exchanger for automotive thermoelectric generator," in *Energy*, vol. 54, pp. 372-377, June 2013.

- [4] Cheng-Ting Hsu, Gia-Yeh Huang, Hsu-Shen Chu, Ben Yu, Da-Jeng Yao, "Experiments and simulations on low-temperature waste heat harvesting system by thermoelectric power generators," in *Applied Energy*, vol. 88, Issue 4, pp. 1291-1297, April 2011.
- [5] Xing Niu, Jianlin Yu, Shuzhong Wang, "Experimental study on low-temperature waste heat thermoelectric generator," in *Journal of Power Sources*, vol. 188, Issue 2, pp. 621-626, March 2009.
- [6] Douglas T. Crane, Gregory S. Jackson, "Optimization of cross flow heat exchangers for thermoelectric waste heat recovery," in *Energy Conversion and Management*, vol. 45, Issues 9–10, pp. 1565-1582, June 2004.
- [7] Baljit Singh, J. Gomes, Lippong Tan, Abhijit Date, A. Akbarzadeh, "Small Scale Power Generation using Low Grade Heat from Solar Pond," in *Procedia Engineering*, vol. 49, pp. 50-56, 2012.